Research Article

Jiyan Chen, Ruidong Yang*, Jie Zhang, and Jinxing Chao

Occurrence of yttrium in the Zhijin phosphorus deposit in Guizhou Province, China

https://doi.org/10.1515/geo-2020-0297
received March 26, 2021; accepted August 20, 2021

Abstract: The Zhijin phosphorite (P)-bearing rare earth element (REE) deposit in Guizhou Province (China) hosts vast ore resources (P: 1.348 billion tonnes; REE: 1.44 Mt). Up to date, the Zhijin phosphorite resource has not been exploited because of the uncertain occurrence of the associated REEs, which hampers mineral processing and extraction. In this study, the structure, the valence state, and the coordination position of Y in the REE-yttrium-rich bioclastic samples from Zhijin were revealed by means of synchrotron radiation X-ray absorption fine structure analysis. The results show that the Y occurs as Y(III) in the samples, and that the form of Y is different from the Y_2O_3 form in standard xenotime samples. Yttrium in the samples was in a complex coordination position without Y–O–Y bonding, and the Y–O bond lengths range widely without clear patterns. We suggest that Y in the samples is surrounded by organic or macro-molecular compounds, rather than in inorganic ones. Thus, Y in collophanite is unlikely to be in the form of isomorphism.

Keywords: rare earth element, elemental occurrence, phosphorite, yttrium, synchrotron radiation XAFS analysis

1 Introduction

Rare earth metal is a strategic material widely used in many high-tech industries and is critical to the future prosperity of humanity. At present, the global production of heavy rare earth elements (HREEs) comes mainly from the ion-adsorbed rare earth ore, and exploring HREEs in phosphorite represents a new way to tackle the global HREE supply challenge [1,2]. A large number of phosphate deposits [3] were discovered in the Ediacaran and Early Cambrian Yangtze platform in South China. Previous studies [4–8] showed that these phosphorite deposits are REE bearing (Figure 1), some of which containing relatively high total (∑) REE contents, such as the Xinhua (aka. Zhijin) (∑REE = 242.92–1059.59 ppm, avg. 611.27 ppm), Kaiyang (∑REE = 42.96–399.5 ppm, avg. 176.1 ppm), Wengan (∑REE = 11.89–223 ppm, avg. 67.4 ppm) [9], Kunyang (∑REE = 5.97–332.62 ppm, avg. 130.16 ppm) [10], as well as the Bahuang (in Tongren) (∑REE = 197.9–1013.35 ppm, avg. 768.08 ppm), Songlin (in Zunyi) (∑REE = 500.33 ppm) [11], and Jingxiang (∑REE = 27.73–157.97 ppm, avg. 93.86 ppm) [12]. According to statistics, the ∑REE content of the Xinhua deposit is higher than that of many Ediacaran to Early Cambrian deposits, especially for the Y content (accounting up to 45% of the total ∑REY). In addition, the ∑REE content is positively correlated with that of P_2O_5 [11,13].

The Xinhua ore district (in Zhijin P deposit) is located southwest of the Zhijin county with high transport accessibility. The ore bodies are mainly distributed along the west limb (close to the axis) of the northeast–southwest-trending Guohua anticline. Structural geology is dominated by transtensional faulting and local small structures. The ore district contains four ore sections, namely Gaoshan, Gezhongwu, Guohua, and Daga. These ore sections are all located on the limbs of the Guohua anticline, and the major prospect locations are shown in Figure 2. Stratigraphy (from bottom up) is the Dengying Formation (Fm.) dolomite, Gezhongwu Fm. sandy phosphorite, bioclastic dolomitic phosphorite, and Niutitang Fm. black shale.

In this study, we studied the profiles with large ore resources, including the Gezhongwu (Figure 3a and c), Guohua (Figure 3d–f), and Majiaqiao (Figure 3b). We observed the vertical change in lithology, color, and sedimentary structure, and performed the sampling in certain spacing.

* **Corresponding author: Ruidong Yang,** College of Resources and Environmental Engineering, Key Laboratory of Karst Georesources and Environment, Ministry of Education, Guizhou University, Guiyang 550025, China, e-mail: ruidong321@outlook.com
Jiyan Chen, Jinxing Chao: College of Resources and Environmental Engineering, Key Laboratory of Karst Georesources and Environment, Ministry of Education, Guizhou University, Guiyang 550025, China
Jie Zhang: College of Mining, Guizhou University, Guiyang 550025, China

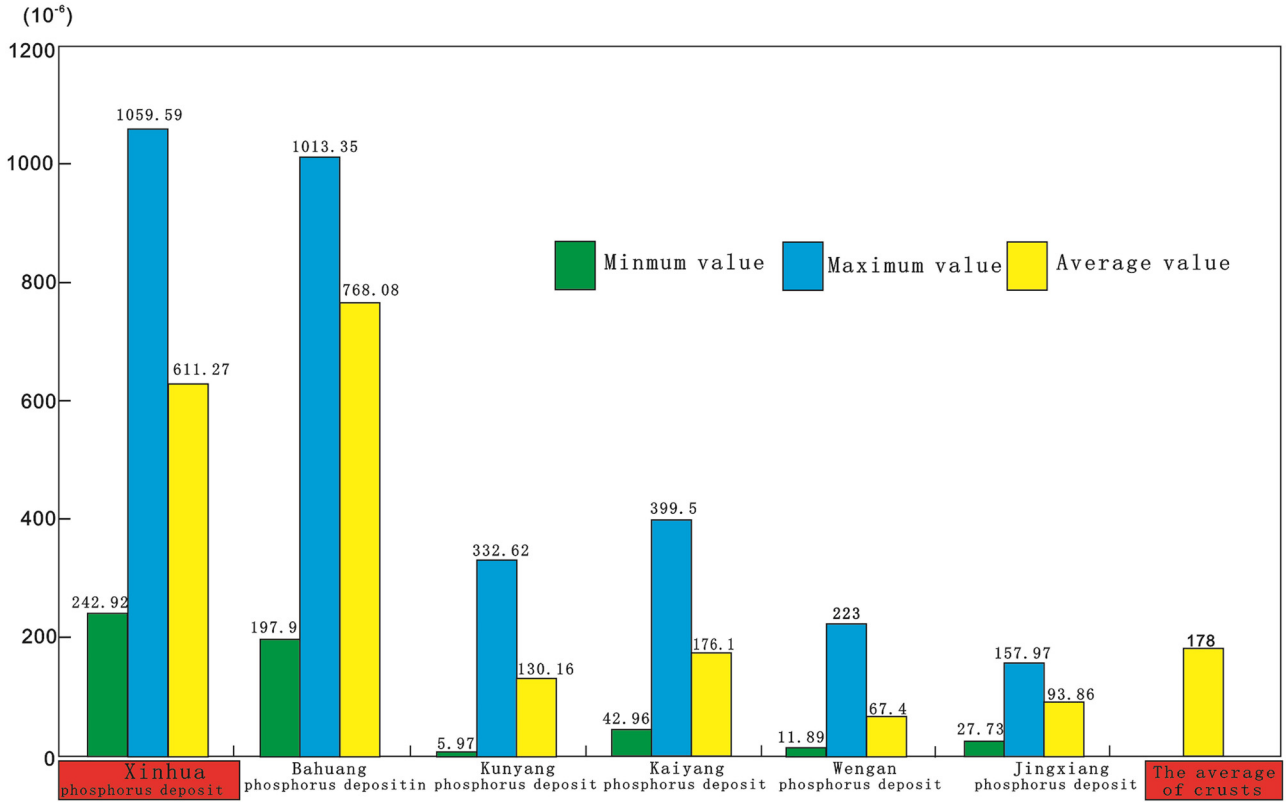

Figure 1: Statistics of REE content in typical phosphate deposits (data source listed above).

Major ore types at Zhijin are dark-/light-gray bioclastic-bearing dolomitic phosphorite (dominant) and brecciated phosphorite [14,15], with the former displaying (inter) layered and banded structure (Figure 4a and b). Bioclasts in the biophosphorites are mainly dominated by small shells (Figure 5a–e), including Zhijinites and hyolithes spicules (Figure 5a) and algal biocide (Figure 5e). Samples from the top of the ore layer contain higher Si contents, and subrounded P-bearing lithics are occasionally found. This not only indicates the complex formation of the P deposit, but also demonstrates the major influence on the occurrence, enrichment environment, and distribution patterns of REEs.

As aforementioned, the REE occurrence in the Zhijin P ores remains to be investigated. The REE occurrence refers to the physicochemical state and their combination with other coexisting elements in a particular stage of the REE migration history. The state of occurrence includes the phase (gas, liquid, solid), the type and form of compounds, the bond type, and the physicochemical features of the valence and coordination position in the crystal lattice.

Research on phosphorite-associated REE has attracted increasing attention in recent years. Previous studies suggested that REEs exist mainly as ion adsorption state (e.g., REE deposits in the Jiangxi granite weathering crust), independent minerals (Bayan Obo REE deposit), or isomorphism in minerals and rocks [16].

As supported by X-ray diffraction (XRD), electron probe microanalysis (EPMA), and inductively coupled plasma-mass spectrometry (ICP-MS) analyses on the REE occurrence at Zhijin, it is concluded that the REEs in phosphorite exist mainly as isomorphism in the carbonate–fluorapatite lattice [10,16–24]. The isomorphic occurrence is likely led by the phosphate–carbonate–fluorapatite crystals in phosphorite, which have open hexagonal columnar structure. In that case, the Ca^{2+} and REE ionic radii are similar and thus REE can enter the crystal via isomorphism. Meanwhile, REEs in phosphorite occur mainly in collophane, most of which exist in apatite as ions and minor adsorbed on clay minerals [4,20,24–27]. This indicates that the REEs in phosphorite do not occur predominantly in independent minerals. Duan et al. studied the Zhijin deposit by means of mineral processing experiment and concluded that the ores contain ion-adsorbing REEs, whose content is lower than those in the form of isomorphism. Besides, scanning electron microscopy (SEM) and energy spectral analysis [19] and ICP-MS analysis [23] found that the REEs do not occur as independent minerals [23], although Liu et al. argued that REEs can occur as cerianite at Zhijin, based on EPMA data [28].

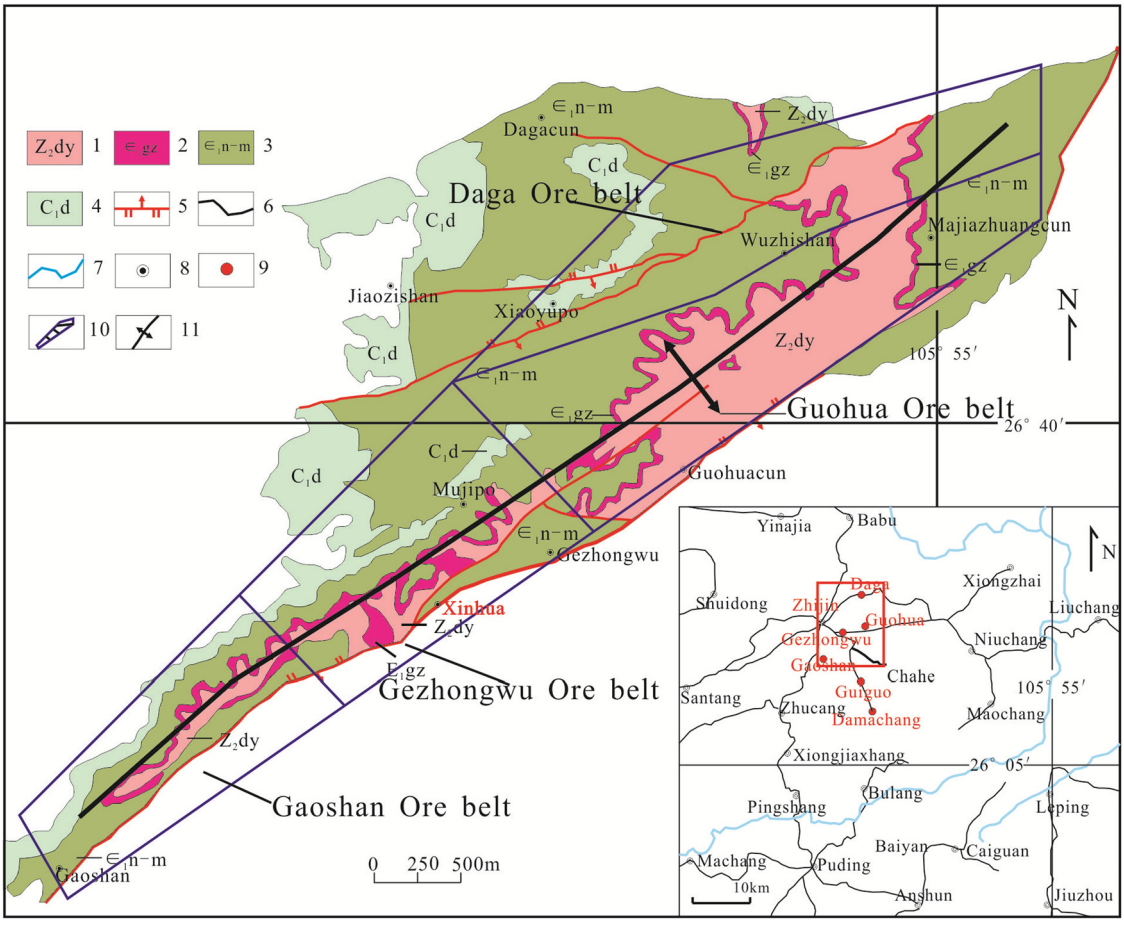

Figure 2: Geographic location and simplified geologic map of the ZhijinXinhua P deposit. Numbers on the map: 1. Dengying Formation; 2. Gezhongwu Formation; 3. Niutitang-Mingxinxi Formation; 4. Dapu Formation; 5. Fault; 6. Roads; 7. Rivers; 8. Name locations; 9. Phosphate prospect; 10. Ore section in the Xinhua P deposit; 11. Guohua-Gezhongwu anticline.

In this study, we applied synchrotron radiation X-ray absorption fine structure (XAFS) experiment to reveal the type of bonding, the valence state, and the coordination information of Y in REE-rich apatite crystals from Zhijin, as well as to elucidate the atomic-scale Y occurrence in phosphorite.

2 Materials and methods

2.1 Sample preparation and standard selection

To achieve more meaningful data, REE-rich phosphorite samples (XL-6-10) from Zhijin (Figure 3a–c) were analyzed instead of whole-rock samples. Mineral trace element geochemistry of the Zhijin REE-bearing phosphorite suggests that the REE contents in both collophanite and bioclastics are high and are closely related to the collophanite content. Probably because of the limited number of samples, pure cellophane samples were not found, and 1#, 2#, and 3# bioclastic samples were selected under heavy fraction lens (Table 1 and Figure 6).

Sample preparation: The bioclastic samples were first grinded to 400 mesh and then spread uniformly on a 20 cm adhesive tape (1–2 cm wide). The thickness was adjusted by folding the adhesive tape.

In this study, standard samples were analytical reagents from the Beijing Fangzheng Rare Earth Science and Technology and the content of Y_2O_3 is 100%. Results of the measured elements were compared with the standard sample data.

2.2 Synchrotron radiation XAFS experiment

The experiment was conducted at the Laboratory of Biomacromolecules (1W1B) of Beijing Synchrotron Radiation Facility, with 2.5-GeV electron storage ring and 150 mA

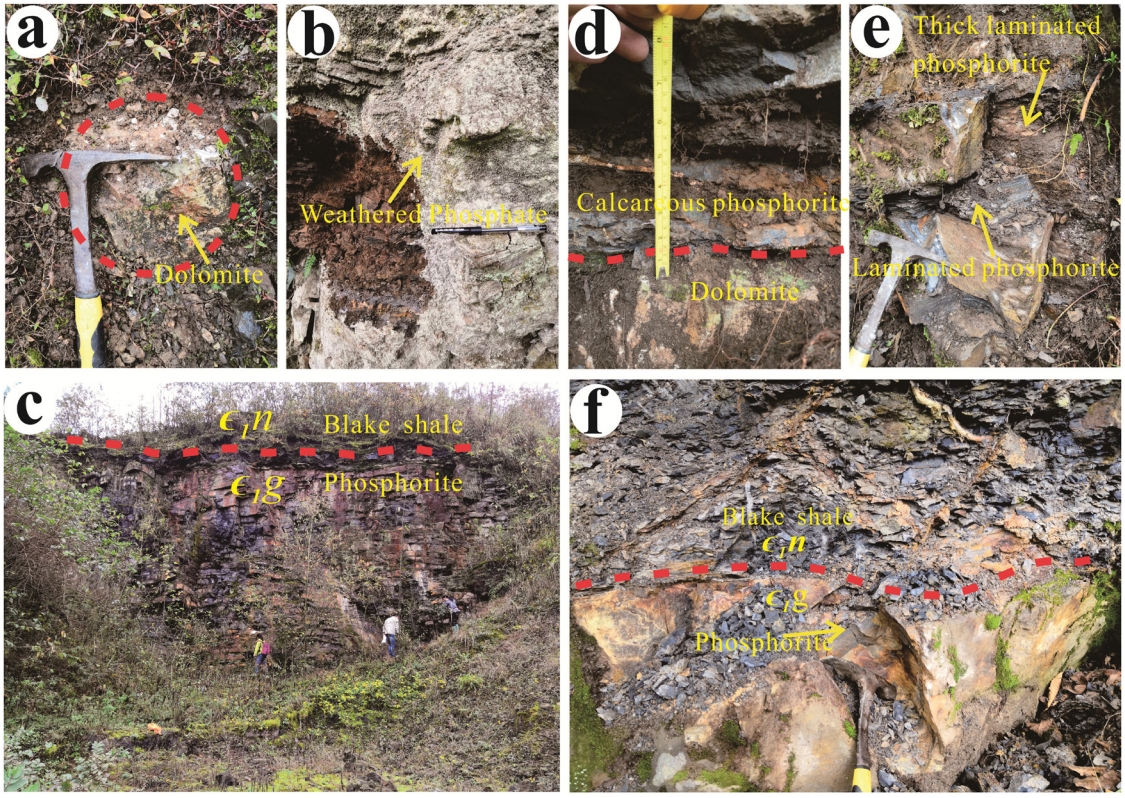

Figure 3: Field geological profile of the Zhijin deposit, Guizhou Province, China. (a) Basal dolomite (Gezhongwu profile). (b) Weathered phosphorite (Majiaqiao profile). (c) Banded dolomitic phosphorite and the overlying Niutitang Fm. black shale (Gezhongwu profile). (d) Basal dolomite in clear contact with calcareous phosphorite (Guohua profile). (e) Thin-medium-bedded cherty phosphorite with banded structure (Guohua profile). (f) Phosphorite in clear contact with the overlying Niutitang Fm. black shale (Guohua profile).

current. Exit-fixed Si (111) double-crystal monochromator was adopted. K-absorption edge (17,038 eV) of Y in Y-bearing minerals was analyzed by using the fluorescence XAFS analysis. Pure Ar gas was used as the absorbing gas in the pre- and post-ionization chambers and Lytle ionization chamber. The fluorescence XAFS technique is highly sensitive and can measure trace element contents down to ppm, Zhang and Chen concluded that the La and Y contents account for about 1–5% (qualitative analysis) of individual mineral dolomite, as determined by SEM analysis of the REE-bearing Zhijin phosphate ores [18–22]. Thus, the REE requirements of fluorescence XAFS experiment can be met in our phosphate ores.

For the fluorescence extended XAFS analysis, the elemental compositions of the standard (REE oxides) were compared with those of the samples. The fluorescence XAFS data were processed with the Athena software to generate the X-ray absorption near-edge structure

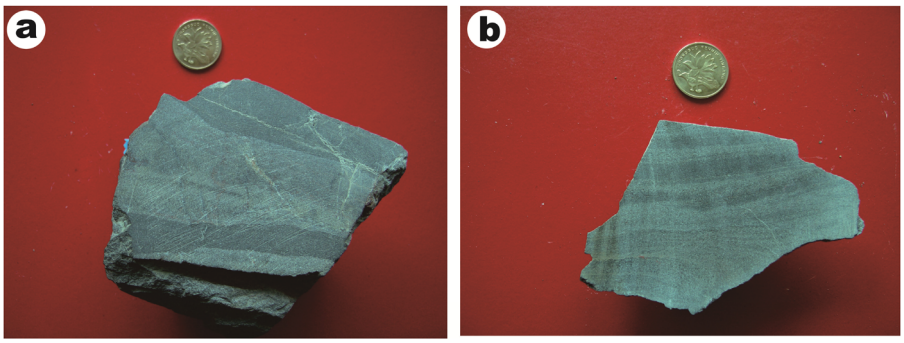

Figure 4: Hand specimen photos of phosphate ores from Zhijin, Guizhou Province: (a) collophane-rich sample; (b) dolomite-rich sample.

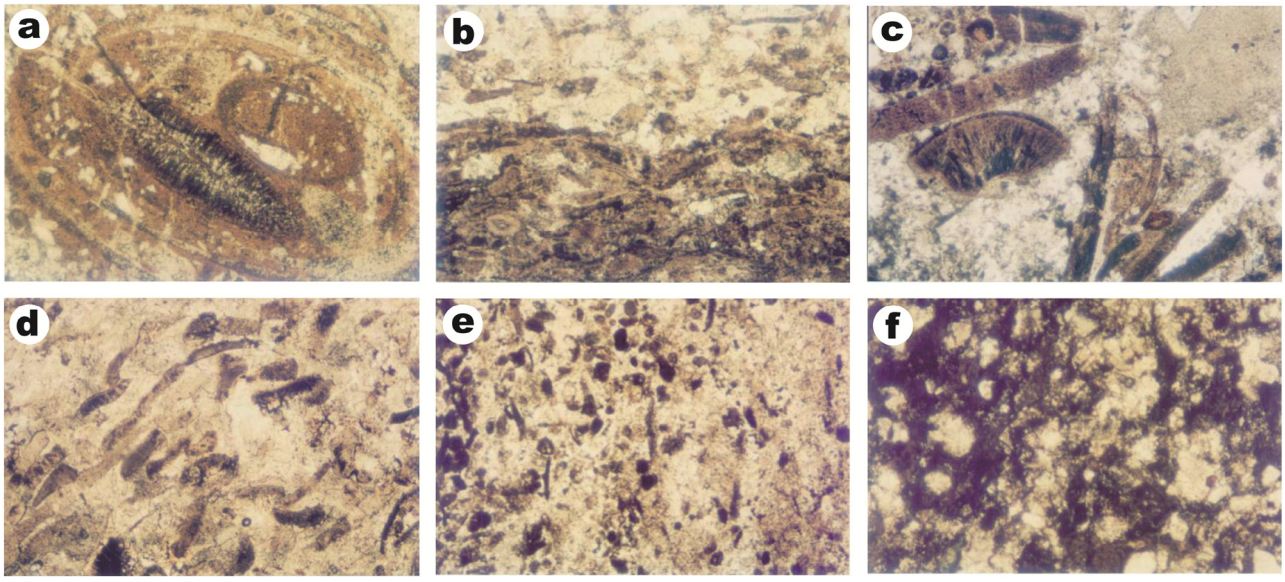

Figure 5: Thin-section microphotographs of the Zhijin phosphate ore, showing microstructural features (plane-polarized transmitted light). (a) Bioclastics in concentric rings (XL-6-10, 5 × 10); (b) bioclastics in radial and drusy form (XD-6-2, 5 × 10); (c) bioclastics show lineation and zoning (XL-6-10, 5 × 10); (d) numerous stripped bioclastics (XL-L-1, 5 × 10); (e) rounded algae fossils in siliceous cement; (f) few bioclastics in this more silicic and phosphoric sample (W-X2, 10 × 10).

Table 1: REE content of fossil and phosphorite in REE-bearing phosphorus rocks in Xinhua, Zhijin County, Guizhou (ppm)

Minerals	Bioclast 2#	Bioclast 3#	Dolomite	Phosphate
La	117.50	113.70	127.30	316.10
Ce	75.64	66.59	73.68	184.35
Pr	17.93	18.32	20.64	51.84
Nd	78.60	80.23	90.93	25.96
Sm	13.86	13.95	15.77	39.72
Eu	3.21	3.26	3.60	8.83
Gd	16.50	16.50	18.40	46.50
Tb	2.31	2.36	2.57	6.46
Dy	14.31	14.75	16.30	8.69
Ho	3.08	2.97	3.51	8.21
Er	8.48	8.17	9.55	21.80
Tm	8.48	8.17	9.55	21.80
Yb	1.02	0.99	1.16	2.46
Lu	5.29	4.99	6.26	12.46
Y	0.72	0.69	0.76	1.57
∑REE	543.74	524.07	587.72	1431.50

Note: Individual minerals were analyzed with ICP–MS at the Institute of Geochemistry, Chinese Academy of Sciences [4].

(XANES) spectra. The spectra were compared with those of the standard, and the structural characteristics of the REE materials were obtained. After processing the XANES spectra with the Athena software (via first derivative), the REE valence features were obtained. Afterward, analysis of the form of REEs was conducted on the XANES spectra, which yielded partial REE structural features of the samples.

Since 1993, various reports were made on the XAFS and XANES spectra [29–34], which emphasized the application of XAFS and XANES spectra in mineralogy, petrology, and metallogeny. Besides, Peng et al. (1999) also investigated the geochemical application of synchrotron radiation X-ray absorption spectra. These authors considered that for the type of trace REE compositions in minerals, the valence state, the coordination position, and the bond features are critical but also very hard to constrain (e.g., Au, Ag, As, and P occurrence). This issue, nonetheless, can be resolved with synchrotron radiation X-ray absorption spectra. Amhed and Thomas conducted synchrotron radiation X-ray absorption spectral analysis on the CeO_2 structure features and yielded values for parameters such as the Ce–O bond length [35]. Similar XANES analysis was conducted on the As occurrence in the tailing of a particular mine, and showed the three As valence states [33,36]. Meanwhile, Manceau et al. conducted synchrotron radiation XAFS on the REE occurrence in manganese nodules and suggested that the Ce occurs as Ce(IV) instead of Ce(III) [37].

All in all, previous synchrotron radiation XANES studies have yielded certain achievements, suggesting that this technique can differentiate and quantitatively analyze the mineral trace REE composition types, valence state, coordination position, and bonding features. This

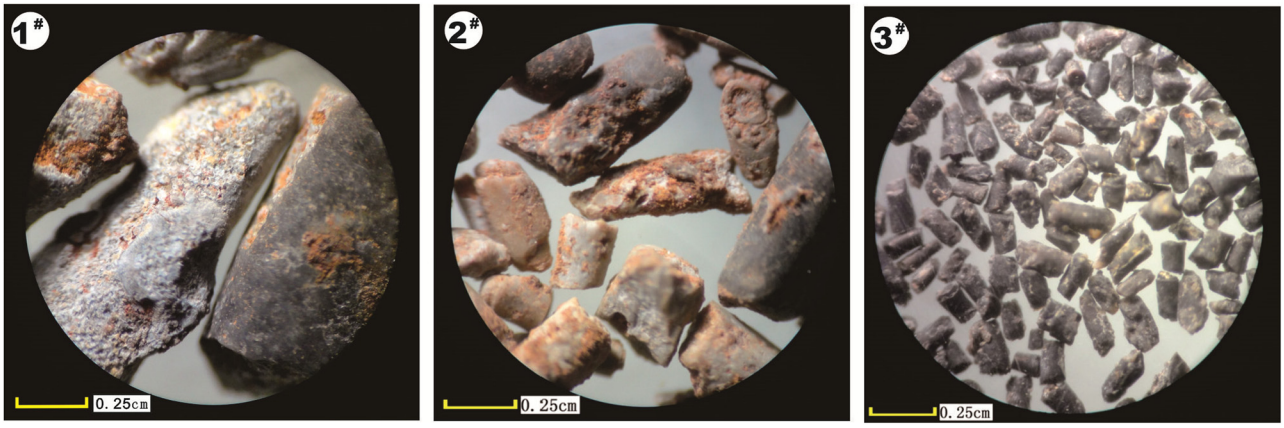

Figure 6: Photos of (from left to right) Nos. 1, 2, and 3 bioclastic samples.

can be used to investigate the REY occurrence in the Zhijin REE-bearing P ores.

XAFS experimental principle, shown in Figure 7, I_0 is the incident X-ray intensity, X-ray permeates the front detector to the sample of thickness d. The detector D_f and the sample is set at 45°, fluorescence signal is received with uniform thick sample ($u_T d < 1$), the fluorescence intensity can be expressed as

$$I_f = \frac{\Omega}{4\pi} \cdot I_0 \cdot w_{fA} \cdot \frac{u_A(E)}{u_A(E) + u_T(E_f)}, \tag{1}$$

$$\text{XAFS signals: } S = \frac{\partial(I_f/I_d)}{\partial u_A} \cdot \Delta u_A = \frac{I_0}{I_d} \cdot \frac{w_{fA} \cdot \frac{\Omega}{4\pi} \cdot \Delta u_A}{u_T(E) + u_T(E_f)}. \tag{2}$$

(Note: w_{fA} = fluorescence yield, Ω = stereoscopic acceptance angle of fluorescent detector (D_f), E = energy of the incident X-ray, E_f = energy of the fluorescent X-ray, $u_A(E)$ = absorption coefficient of the element A to be measured, $u_B(E)$ = absorption coefficient of all the other atoms in the sample and the absorbed atoms, $\mu_T(E_f)$ = total absorption coefficient at the fluorescence energy).

The signal contains not only the XAFS signal of the structural information of the measured elements, but also the fluorescence spectra of the other elements in the sample and the background signal scattered by the elastic and inelastic X-rays. However, the background signal and the fluorescence spectrum were separated on the energy axis. During the incident light scanning, the fluorescence energy spectrum is constant and the intensity changes with the incident light energy to form a scattered peak. The scattered peak shifts to the high-energy end with increasing incident light energy. Fluorescence detection mode inhibits the background signal and increases the ratio of the measured element fluorescence signal, to obtain the absorption spectrum of the structural information of the measured elements in the sample.

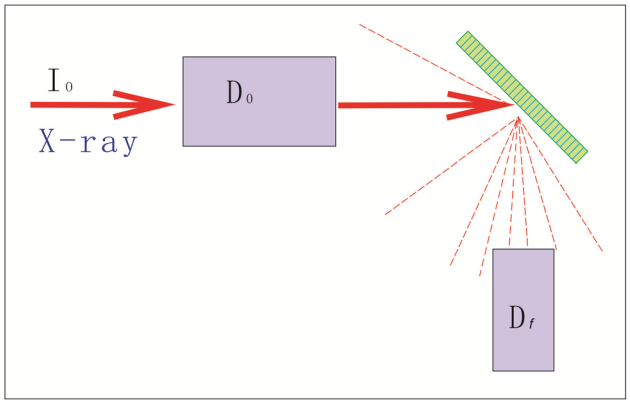

Figure 7: Schematic diagram of the fluorescence method.

3 Results

Owing to the low Y content of the samples (below 1,000 ppm), only the XANES data were obtained by the fluorescence analysis. Compared with standard Y_2O_3 oxides, the first peak value is offset from the main peak, indicating that the structural form of REYs in the samples differs from that of the standard (Figure 8). The second peak value shows that the corresponding peak values of the Y_2O_3 in these three samples are clearly lower than those of the standard. Although the Y_2O_3 peak value in No. 1 sample is closest to that of the standard, the spectral lines disappear gradually and are jagged. The corresponding spectra of Y_2O_3 in No. 2 sample are more distinct but jagged, implying that both Nos. 1 and 2

samples contain impurities. The spectral lines of No. 3 sample are close to those of the standard and are smooth and show strong extended X-ray absorption fine structure (EXAFS) signals. This indicates that the sample is relatively pure.

Figure 9 illustrates the EXAFS results of No. 3 bioclastic sample, and shows that the Y valence in the samples do not change much and is similar to that of the standard. This indicates that the Y in our samples occurs as Y(III).

In Figure 8, it is shown that the local structure of Y in the samples is quite different from the Y_2O_3 form in the standard. The Y in the samples is in a complex coordination environment without such Y–O–Y bonding, and the Y–O bond length is slightly shorter with a wider distribution, which indicates that the internal local environment of Y in the samples is markedly different from that of Y_2O_3 in the standard, and its coordination environment of the former is more complex. There are several Y–O bonds with various lengths close to 2.1 A, and the peak corresponding to the Y–O–Y bond length position disappears. This indicates that the ambient local environment of Y in the samples is clearly different from that of Y_2O_3 in the standard, and that no similar long-order range of crystals is present. This is consistent with the XANES results, which demonstrates that the REYs in the Zhijin REE-bearing phosphate ores do not occur in an inorganic form.

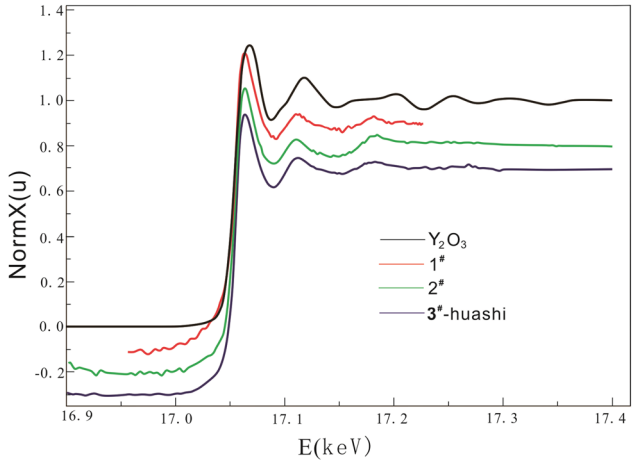

Figure 8: Y-K-edge XANES spectra.

4 Discussion

We have used XRD, SEM, phase analysis, and other means to search the local environment of Y in phosphate ore, during my master's degree study with my teacher, Professor Zhang Jie, but did not get the expected results. Therefore, this study adopts XAFS innovative experiment for quantitative research and finds some differences with previous research results. The results show that the local form of Y was different from the Y_2O_3 form in complex coordination environment and that Y–O–Y bonding is absent. Besides, the Y–O bond length has no obvious change but has a wide distribution, which indicates that Y in the samples is surrounded by organic or macromolecular compounds instead of inorganic materials. Thus, the organic extraction can be an effective method in the separation and extraction of the REY resource in the Zhijin REE-bearing phosphate ores.

Our results on the REY occurrence in phosphorites differ from those reported by previous studies, in that the REEs exist in collophanite in the form of isomorphism.

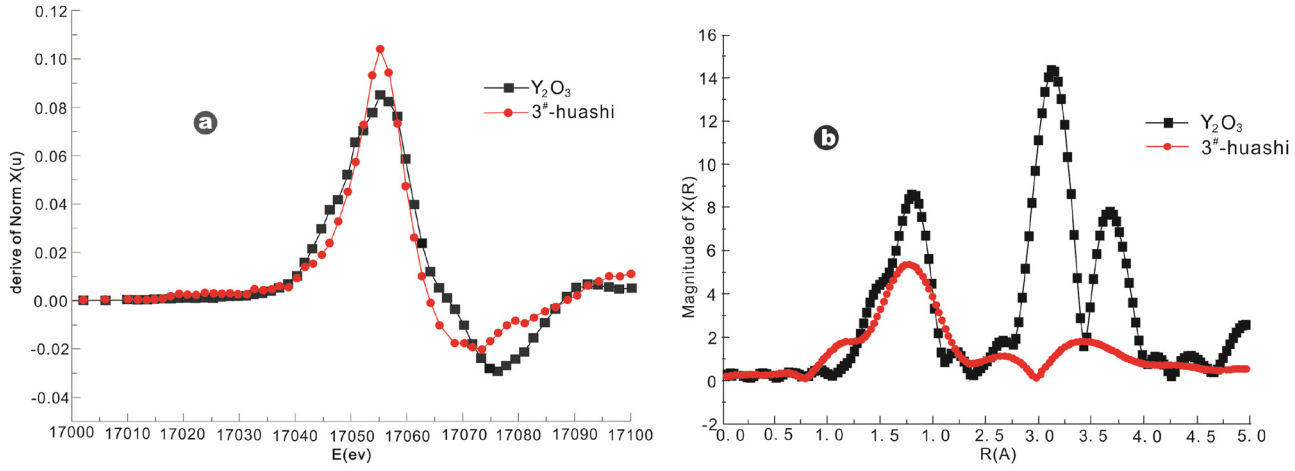

Figure 9: EXAFS plot (a and b).

However, it does not preclude the other forms of REE occurrences as proposed in previous studies.

5 Conclusion

The results show that the valence of Y in the samples was 3^+, and the local form of Y is different from the Y_2O_3 form in standard xenotime. Yttrium in the samples is in a complex coordination environment without Y–O–Y bonding, and the Y–O bond length has no obvious change but a disperse distribution. It is indicated that Y in the samples is surrounded by organic or macromolecular compounds, but not by inorganic materials. Through microscopic investigation of Y (occurrence, valence state, and local environment) in P ore minerals, it is found that organic extraction is more effective for REEs in the Zhijin REE-bearing phosphate deposit. Shortfalls of this work are the limitation of the sample separation conditions. This early-stage experiment has only picked bioclastic samples, and the REY-related dolomite and collophane single-mineral samples are yet to be separated or analyzed.

Acknowledgments: We are grateful to Professor Zheng Lirong from the Beijing Electron Positron Collider National Laboratory (Institute of High Energy Physics, Chinese Academy of Sciences) for helping with the experiment.

Funding information: The project was supported by the National Natural Science Foundation of China (41862002).

Conflict of interest: Authors state no conflict of interest.

References

[1] Emsbo P, Mclaughlin PI, Breit GN. Rare earth elements in sedimentary phosphate deposits: solution to the global REE crisis? Gondwana Res. 2015;27(2):776–85.
[2] Hein JR, Koschinsky A, Mikesell M, Mizell K, Glenn CR, Wood R. Marine phosphorites as potential resources for heavy rare earth elements and Yttrium. Minerals. 2016;88(6):1–22.
[3] Huan C, Shuhai X, Chuanming Z, Yongbo P. Phosphogenesis associated with the Shuram excursion: petrographic and geochemical observations from the Ediacaran Doushantuo formation of South China. Sediment Geol. 2016;341(1):134–46.
[4] Chen JY, Yang RD. Analysis on REE geochemical characteristics of three types of REE-rich soil in Guizhou Province, China. J Rare Earths. 2010;28:517–22.
[5] Mao T, Yang RD, Mao JR. Research on carbon and oxygen isotopes in phosphorus-bearing rock series of the late Neoproterozoic-early Cambrian Taozichong formation in Qingzhen City, Guizhou Province, Southwest China. Chin J Geochem. 2014;33(4):439–49.
[6] Chen JY, Yang RD, Wei HR, Gao JB. Rare earth element geochemistry of Cambrian phosphorites from the Yangtze region. J Rare Earths. 2013;31:101–10.
[7] Yang BQ, Zhang XP. Analysis of global rare earth production and consumption structure. Chin Rare Earths. 2014;35(1):110–8.
[8] Xiao CY, Zhang ZW, He CZ. The depositional environment of Ediacaran phosphorite deposits, South China. Bull Mineral Petrol Geochem. 2018;37(1):121–37.
[9] Shi CH. Formation of phosphorite deposit, breakup of Rodinia supercontinent and biological explosion. Guiyang: Institute of Geochemistry, Chinese Academy of Sciences; 2005. p. 25–6.
[10] Yang WD, Qi L. Geochemical characteristics and genesis of rare earth elements in early Cambrian phosphorite series in eastern Yunnan. Bull Mineral Petrol Geochem. 1995;14(4):224–7.
[11] Xie H, Zhu LJ. The modes of occurrence of rare earth element in phosphorite of Meishucun stage of Cambrian in Guizhou. China Min Mag. 2012;21:65–70.
[12] Luo DK. Geochemical characteristics and genesis of Jingxiang phosphorite deposit in Hubei Province. Beijing: China University of Geosciences; 2011. p. 39–9.
[13] Zhang YB, Gong ML, Li H. The modes of occurrence of rare earth elements in phosphorite of Meishucun stage of Cambrian in Guizhou. J Earth Sci Environ. 2007;29:362–8.
[14] Liu XQ, Zhang H, Tang Y, Liu YL. REE geochemical characteristic of apatite: implications for ore genesis of the Zhijin phosphorite. Minerals. 2020;1012(10):3–22.
[15] Han YC, Xia XH, Xiao RG, Wei XS. Phosphorus deposits in China. Beijing: Geological Publishing House; 2012. p. 410–513.
[16] Neary CR, Highly DE. Chapter 12 – The Economic Importance of the Rare Earth Elements. In: Henderson PBT, editor. Developments in Geochemistry. Elsevier; 1984. p. 423–66.
[17] Kazutaka Y, Hanjie L, Koichiro F, Shiki M, Satoru H. Geochemistry and mineralogy of REY-rich mud in the eastern Indian Ocean. J Asian Earth Sci. 2014;93:25–36.
[18] Zhang J, Chen DL. Scanning electron microscope study of the ore-bearing REE in Xinhua phosphorite, Zhijin, Guizhou. J Mineral Petrol. 2000;20:59–64.
[19] Zhang J, Zhang Q, Chen DL. REE geochemistry of the ore-bearing REE in Xinhua phosphorite, Zhijin, Guizhou. J Mineral Petrol. 2003;23:35–8.
[20] Zhang J, Shun CM, Yang GF, Xie F. Separation and enrichment of rare earth elements in phosphorite in Xinhua, Zhijin, Guizhou. J Rare Earths. 2006;24:413–8.
[21] Zhang J, Sun CM, Gong ML, Zhang T, Chen DL, Chen JY. Geochemical characteristics and occurrence states of the REE elements of the phosphorite in Xinhua, Zhijin, Guizhou. Chin Rare Earths. 2007;28:75–9.
[22] Zhang J, Zhang T, Chen JY. Rare earth elements geochemical characteristics of early phosphorite in Cambrian, Guizhou. Beijing: Metallurgical Industry Press; 2008. p. 1–117.
[23] Duan KB, Wang DH, Xiong XX. A review of a preliminary quantitative study and genetic analysis for rare earth elements of ionic adsorption state in phosphate ore deposit in Zhijin, Guizhou Province. Rock Miner Anal. 2014;28:517–22.
[24] Zhang J, Ni Y, Liang JT. Characteristics of mineralogical technology about medium-low grade bio-chip containing the rare

earth dolomitic phosphorite in Xinhua, Zhijin, Guizhou. J Rare Earths. 2010;28:525–7.
[25] Zhang YB, Zhang BY, Yang SQ, Zhong ZG, Zhou HP, Luo XP. Enhancing the leaching effect of an ion-absorbed rare earth ore by ameliorating the seepage effect with sodium dodecyl sulfate surfactant. Int J Min Sci Technol. 2021;31(6):995–1002.
[26] Chelgani SC, Rudolph M, Leistner T, Gutzmer J, Peuker UA. A review of rare earth minerals flotation: Monazite and xenotime. Int J Min Sci Technol. 2015;25(6):877–83.
[27] Moldoveanu AG, Vladimiros GP. Recovery of rare earth elements adsorbed on clay minerals: II. Leaching with ammonium sulfate. Hydrometallurgy. 2013;131–132:158–66.
[28] Liu SR, Hu RZ, Zhou GF, Gong GH, Jin ZS, Zheng WQ. Study on the mineral composition of the clastic phosphate in Zhijin phosphate deposits, China. Acta Mineralogica Sin. 2008;28:244–50.
[29] Hu TD, Xie AL, Huang DX. Application of XAFSin mineralogy. New research on mineral physics and mineral materials. Beijing: Seismological Press; 1993. p. 16–7.
[30] Peng MN, Li DN. K-edge XANES study on Si and Al from silicate minerals. Guangzhou: Sun Yat-Sen University Press; 1995. p. 6–8.
[31] Peng MN, Li DN, Lin B, Liang JL. Synchrotron radiation X-ray absorption spectra and its application in mineralogy and geochemistry. Bull Mineral Petrol Geochem. 1999;18(1):33–7.
[32] Li DN, Peng MN. K-edge XANES study in silicate glass. Synchrotron radiation technique and application. Beijing: Sciences Press; 1996. p. 122–5.
[33] Li DN, Peng MN. K-edge XANES study on Al from Al_2SiO_5 polytype minerals. Bull Mineral Petrol Geochem. 1997;16:97–8.
[34] Chu BB, Luo LQ, Xu T. XANES study of lead speciation in Duckweed. Spectrosc Spectr Anal. 2012;32(7):1975–8.
[35] Amhed M, Thomas P. Cerium L_{III} EXAFS investigation structure of crystallization and amorphous cerium oxides. Fuel Chem. 2004;49(2):759–61.
[36] Zhu XY, Wang RC, Lu XC, Huang SY. Occurrence of arsenic in shallow shale sulfide ore tailings of Yangshan, Tongling, Anhui Province. Acta Petrolog et Mineralog. 2013;32(6):918–24.
[37] Manceau A, Lanson M, Takahashi Y. Mineralogy and crystal chemistry of Mn, Fe, Co, Ni, and Cu in a deep-sea Pacific polymetallic nodule. Am Mineralogist. 2014;99:2068–83.